EBTS: DESIGN AND EXPERIMENTAL STUDY*

A. Pikin, J. Alessi, E. Beebe, A. Kponou, K. Prelec,
G. Kuznetsov[†], M. Tiunov[†]

Brookhaven National Laboratory, Upton, NY 11973, USA
[†]*Budker Institute of Nuclear Physics, 630090 Novosibirsk, Russian Federation*

Abstract. Experimental study of the BNL Electron Beam Test Stand (EBTS), which is a prototype of the Relativistic Heavy Ion Collider (RHIC) Electron Beam Ion Source (EBIS), is currently underway. The basic physics and engineering aspects of a high current EBIS implemented in EBTS are outlined and construction of its main systems is presented. Efficient transmission of a 10 A electron beam through the ion trap has been achieved. Experimental results on generation of multiply charged ions with both continuous gas and external ion injection confirm stable operation of the ion trap.

INTRODUCTION

The ability to generate high currents of ions with charge states sufficient for single turn injection into the Booster ring of the Alternating Gradient Synchrotron without preaccelerating and subsequent stripping was the main feature of the proposal to begin an EBIS-based project for a new heavy ion injector for RHIC at BNL [1]. The required intensity of $3x10^9$ ions of Au^{35+} per pulse can be satisfied with an electron beam current of 10 A, energy 20 keV, and trap length 1.5 m, assuming 50% neutralization of electron space charge in a trap by the ions and 20% of Au^{35+} ions in the charge state spectrum. RHIC requirements for the parameters of ion beams extracted from EBIS can be satisfied with the electron beam current density in the trap region of 600 A/cm^2, which provides a repetition rate of the RHIC EBIS of 10 Hz for generation of ions Au^{35+} assuming an efficiency of ion confinement in the volume of the electron beam of about 60%. The possibility of few-turn injection into the AGS Booster requires an ion pulse duration of 10-40 μs. The peak total ion current at the EBIS exit in this case would be as much as 8 mA, and the ion optics should be capable of transmitting this beam to the RFQ with minimal losses.

Initial studies were performed on the BNL TestEBIS, the first EBIS operated at BNL [2]. Subsequently to study problems of generating a 10 A electron beam, maintaining high vacuum in multi-amp operation of EBIS, dissipating high power electron beam in electron collector, fast extraction, diagnostics and control, Electron Beam Test Stand (EBTS) has been built in BNL. This device is a half-length, full-electron current prototype of the proposed RHIC EBIS. The main parameters and computer

simulations of generation, transmission and collection of 10 A electron beam of the EBTS have been published in [3,4]. It has been used for electron and ion beam tests as well as for development of diagnostics and controls.

1. DESIGN OF THE EBTS

The main concern in designing EBTS for a 10 A electron beam was stability of the ion-electron system in a trap. Based on available experience of electron beam ion devices (EBISes and EBITes) operating with electron beams below 1A and taking into account known mechanisms of ion heating in the electron beam, it was decided to use the following approaches to reduce ion heating and the rate of ion losses:

- Reduce coupling of the electron beam with drift tubes and increase the allowable amplitude of radial oscillations of ions by increasing the inner diameter of drift tubes to 31 mm (which is more than 3 times larger than in most EBISes).
- Reduce the quality of the drift structure as an oscillator by varying the basic dimensions of drift tubes.
- Use a highly laminar electron beam with minimal transverse temperature and moderate current density.
- Suppress the positive feedback in ion heating by reducing the flux of reflected electrons from the electron collector region.

To avoid a lengthy cycle of heating up and cooling down helium cryostat of the superconducting solenoid every time the EBTS has to be vented to atmosphere, the decision was made to have the drift structure at room temperature and solenoid with a warm bore. With the drift structure at room temperature the problem of buildup of gas layers on the walls of drift tubes was also eliminated.

It was decided to use an unshielded superconducting solenoid, because in this case the fringe magnetic field on both sides of the solenoid allows one to lengthen the transition regions of electron beam compression well beyond the edges of the solenoid and use conventional vacuum pumps in these areas.

Using separate bucking coils for the electron gun and electron collector decouples the electron beam launching, compression and collection from the main solenoid. Five sets of external transverse magnet coils allow versatile adjustment of the electron beam transmission in different regions, and their use significantly reduces electron beam losses on elements of the drift structure.

The assembly view of EBTS is presented on Fig.1.

1.1. Electron beam generation and drift structure

Based on the analysis of possible methods of electron beam generation [4] it was found that the requirements for the electron beam could be satisfied with an electron gun, which utilizes the geometry of a coaxial diode with magnetic insulation. A separate magnet coil provides the axial magnetic field for this gun. The gun consists of a convex spherical cathode mounted in a focusing electrode and cylindrical anode. This gun with coaxial configuration of cathode and anode is an inverse version of a magnetron gun. Since only magnetic compression is used to achieve the final electron

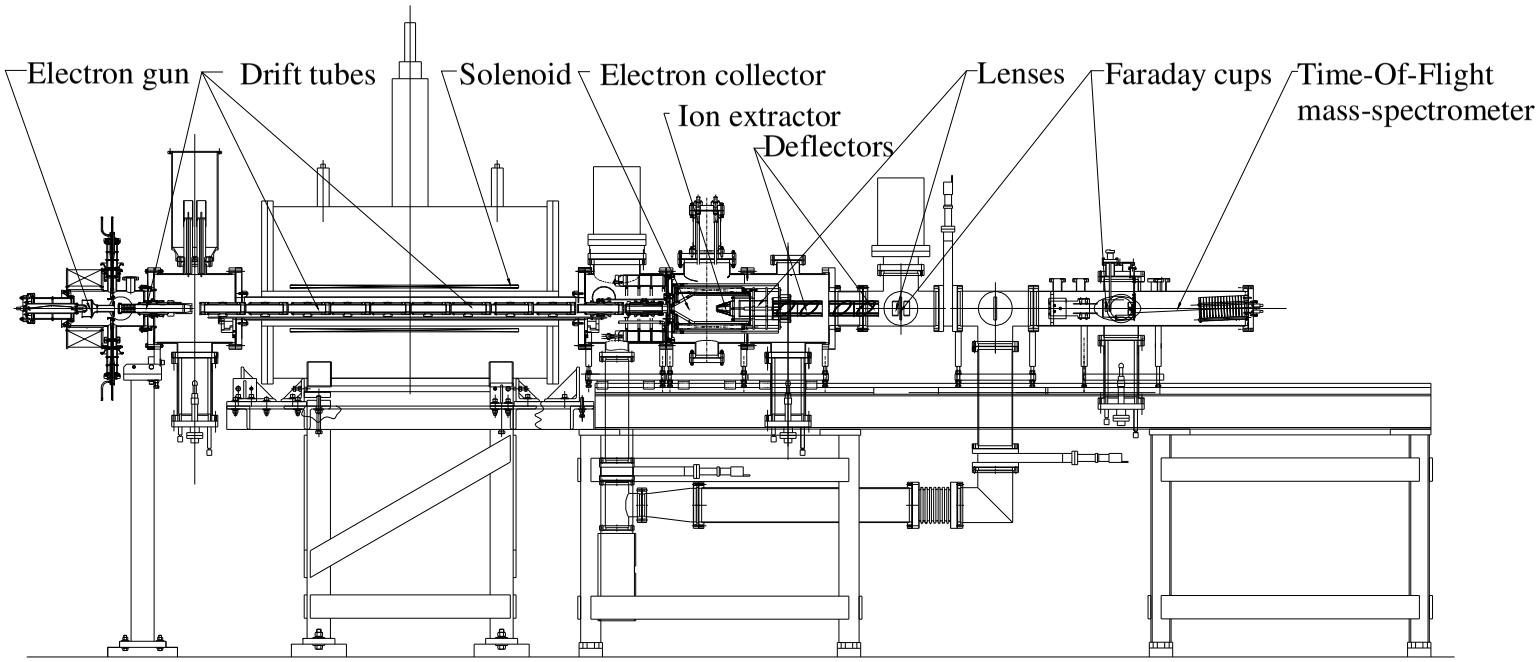

Fig 1. Assembly view of the BNL Electron Beam Test Stand

beam current density it is desirable to have a high emission density from the cathode. On the other hand, the surface of the cathode has to be very smooth, because for this gun configuration most of the acceleration takes place close to the cathode, and its surface roughness directly determines the effective temperature of the electron beam. Deterioration of the cathode within its lifetime should not affect the main parameters of the electron beam. The geometry of the gun with basic dimensions (in mm) is presented on Fig. 2.

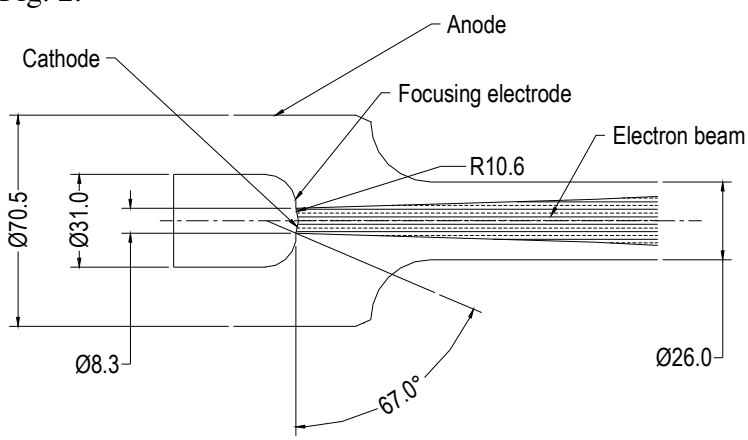

Fig. 2. Geometry of EBTS electron gun

The calculated perveance of this electron gun is $P=1.22\cdot10^{-6}$. The nominal magnet field at the cathode is $B_c=0.16$ T and is produced mostly by the gun coil, with little contribution from the main solenoid. Simulated electron trajectories for the launching of a 13.6 A electron beam are presented on Fig. 3. At 100 mm from the cathode the electron beam has an optical emittance of 3.58 π·mm·mrad, which is 50% of the "thermal" emittance.

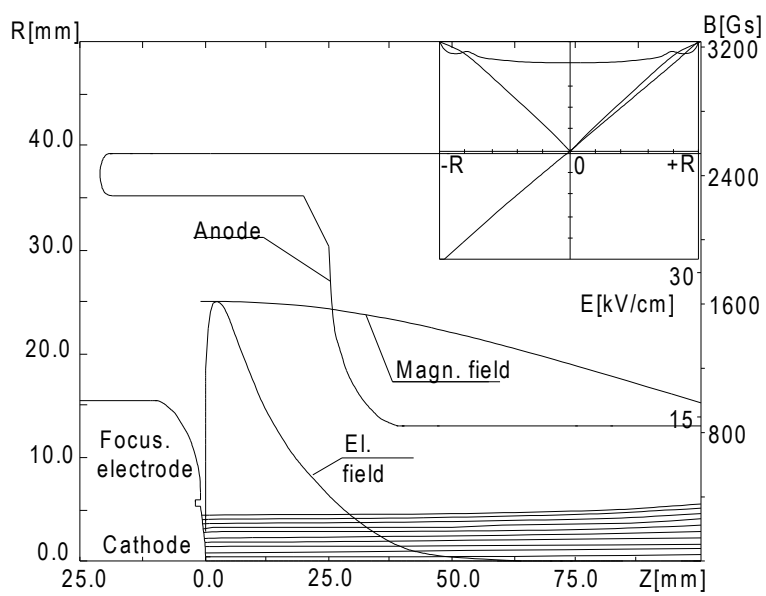

Fig. 3. Simulation of electron beam extracted from the electron gun

Based on available experience with LaB_6 cathodes the actual emittance, which is determined by the roughness and temperature of cathode surface, is approximately 10 times larger. The rotation of the electron beam, defined as a ratio of maximum azimuthal velocity to axial velocity, is 0.037, i.e. the electron trajectories are essentially parallel.

The cathode is manufactured from a single crystal LaB_6. Its lifetime for continuous operation with a current of 10 A is at least 1000 hours without significant degradation of the electron beam quality.

The axial magnetic field of the EBTS is produced by 3 separated coils. A typical field profile and the corresponding electron beam profile are shown in Fig. 4. One can see distinct electron beam radial maxima corresponding to the magnetic field minima. For magnet compression of the electron beam, the current density j(z), at an axial position z, is proportional to the ratio of the magnet field, B(z), at this point to the magnet field on the cathode, B_c: $j(z)=j_c\cdot(B(z)/B_c)$, where j_c is current density on the cathode. The simulated dependence of electron beam current density in the ion trap region on B_c is presented in Fig. 5.

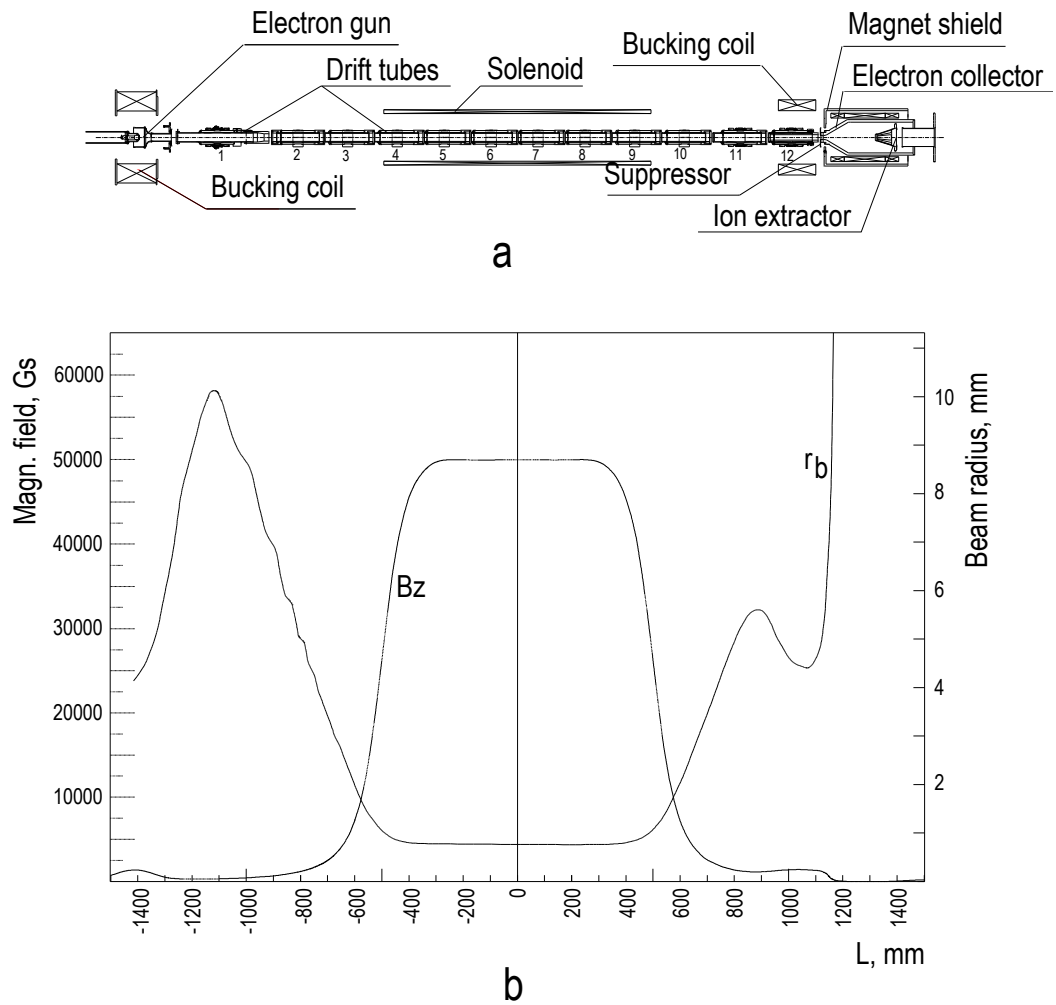

Fig. 4. Electron optical configuration of EBTS (a) and corresponding simulated magnetic field with axial profile of the electron beam (b).

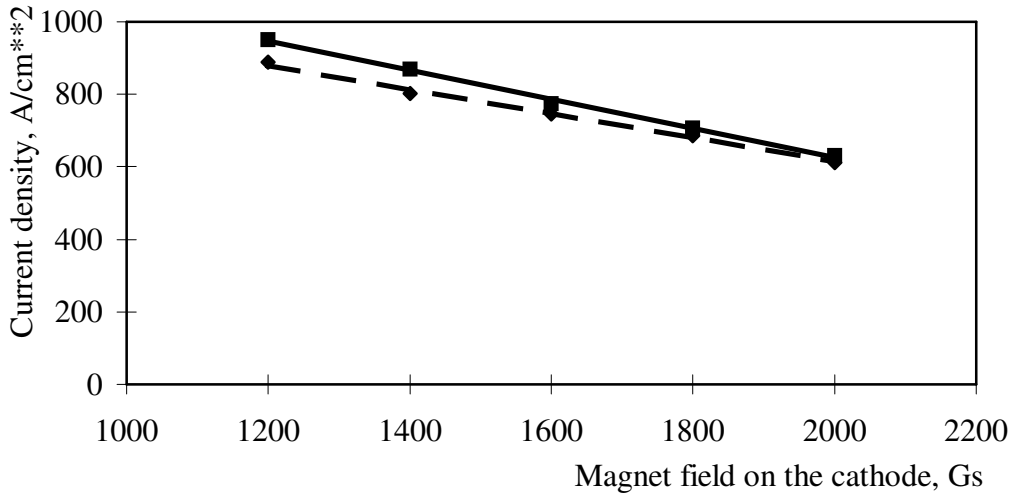

Fig. 5. Dependence of maximum (solid line) and minimum (broken line) electron beam current density (effect of scalloping) on B_c for 13.6 A electron beam. Magnetic field in the trap is B_t=5 T.

By lowering B_c a higher current density electron beam can be achieved in the trap region. However, a consequence is increased scalloping, which leads to a reduced maximum capacity of the ion trap. This occurs because the energy of the electron beam must be raised to avoid virtual cathode formation, thereby reducing the trap region linear charge density. The effect of B_c on minimum potential in the trap is presented in Fig. 6.

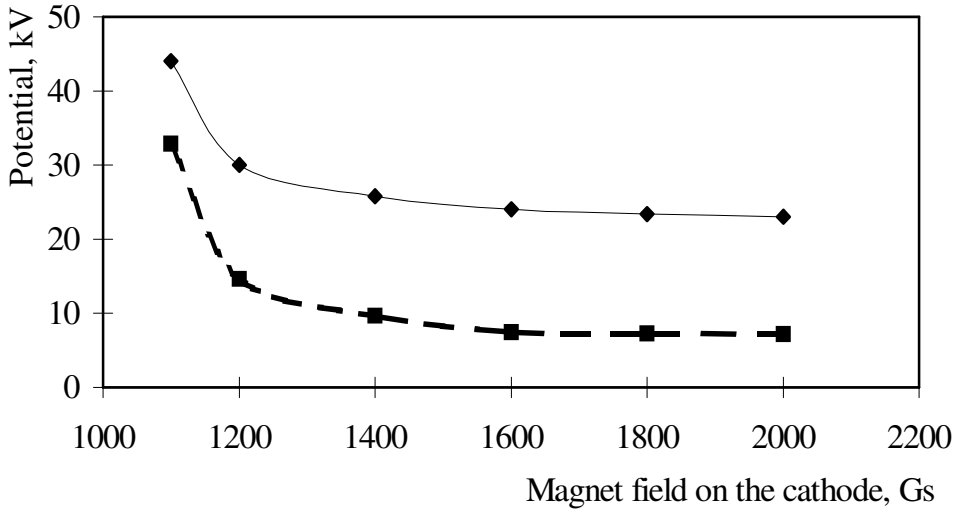

Fig. 6. Critical potentials for virtual cathode formation versus cathode magnetic field B_c. The solid line is the potential applied to the trap region drift tubes and the dotted line is the resulting potential on the electron beam axis. The calculation assumes an uncompensated 13.6 A electron beam in the central drift tube region and a main solenoidal field of 5 T.

Analyzing both dependences, one can conclude that the minimum value of B_c in our case is 1200 G. As one can see, the calculated value of minimum potential on the axis of the 13.6 A electron beam for the nominal value of B_c= 0.16 T is less than 10 kV. This means that the EBTS requirement for a minimum energy of 20 keV for a 10 A electron beam can be met with a good safety factor.

The drift tube structure consists of 12 insulated stainless steel tubes. It was tested without magnetic field up to 40 kV. The average inner radius of the drift tubes is 32 mm and varies slightly from tube to tube. The lengths of tubes vary between 140 and 170 mm. The gaps between tubes vary between 4 and 7 mm. Presently, four central drift tubes form an ion trap of length 71 cm. Drift tubes 2 -10 and their corresponding electrical leads are mounted on a semicylindrical support, which is insulated from the solenoid bore and can be removed and reinstalled without realignment of the drift structure.

The superconducting solenoid, manufactured by Oxford Instruments, Inc., is 1 m long and has a warm bore inner diameter of 154 mm. The maximum operating field is 5 T, with a 5.5 T test field. It can operate in persistent mode with period between refilling of liquid helium about 3 weeks.

1.2. Electron collector

The electron collector for EBTS was designed for maximum average electron beam power dissipation of 50 kW. The total internal area is 1000 cm^2 and inner diameter of the cylindrical part is 114 cm. The diameter of the entrance aperture is 18 mm. The electron beam power is removed by water flow in cooling channels with an equivalent diameter of 6.4 mm. There are 4 parallel loops, each with length 1.8 m. For a pressure drop across the cooling channels ΔP_{EC} =0.275 MPa, the total measured water flow is Q_{EC}= 0.27 l/s. The electron collector design is presented in Fig. 7.

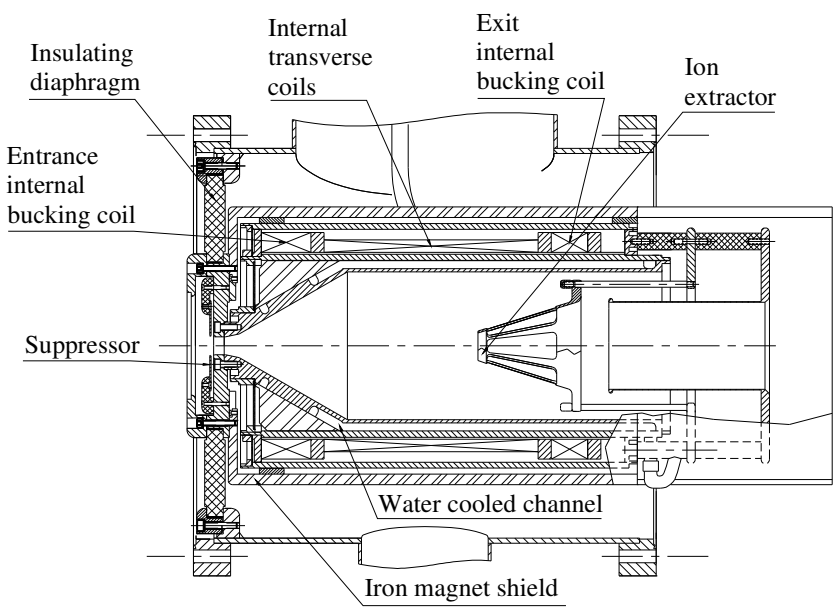

Fig. 7. Assembly view of the electron collector mounted in the vacuum chamber.

The electron collector is located in vacuum and consists of two separate coaxial, sealed chambers: an inner chamber, which contains water-cooling channels and an outer chamber under atmospheric pressure, which contains two bucking coils, two sets of transverse magnet coils for steering or rotating the electron beam inside the collector, a heater and thermocouple. Electric power dissipated in the internal coils is removed by water flow in the cooling channels. The collector is partially surrounded by an iron magnetic shield. The magnetic field at the entrance to and inside the electron collector is adjusted using a coil (not shown on this picture) located in front of the collector entrance, in the fringe field of the main solenoid. The collector's two internal bucking coils can be used for additional correction of the magnetic field if necessary. The collector is mounted on a ceramic ring to provide electrical insulation up to 30 kV. In our present configuration the collector is held at ground potential through a current measuring circuit.

Electron beam trajectories in the collector region are presented in Fig. 8. This simulation as well as simulation of the electron gun was performed with the computer program SAM [5].

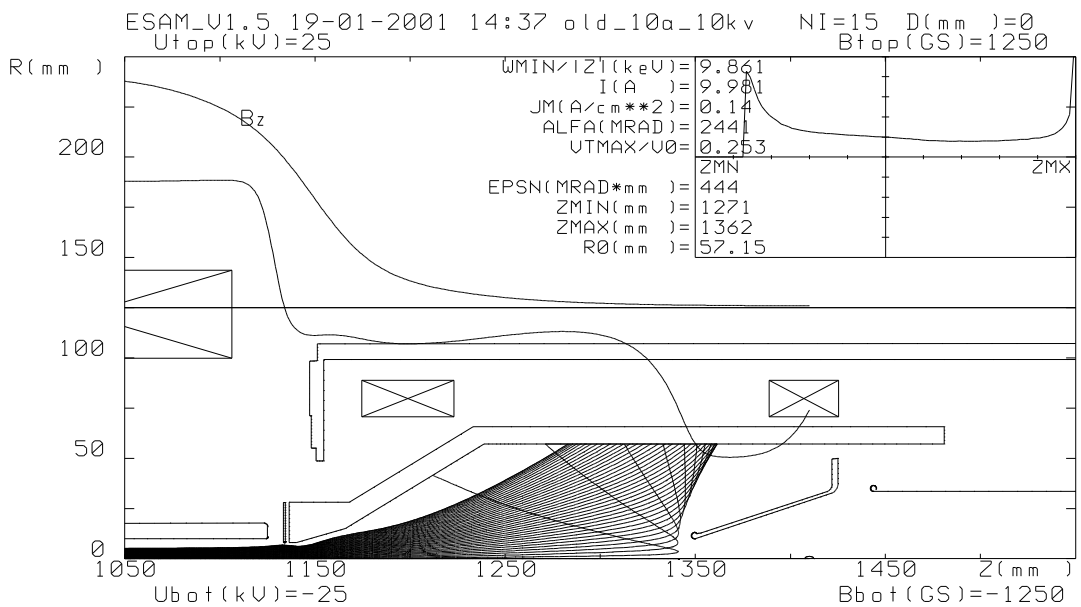

Fig. 8 Simulation of the electron beam transmission in the electron collector.

The electron beam is distributed on the collector surface non-homogeneously: its density is higher in areas close to entrance and decreases sharply towards the collector exit. The main concern in the collector design and operation is creating proper conditions for removal of electron beam power without creating a vapor layer on inner surfaces of cooling channels, which would dramatically reduce the heat transfer to the cooling water. With an electron current of 10 A and energy of 13 keV the local power density can reach q_{max}= 700 W/cm^2. This value exceeds the expected critical power density for continuous operation by a factor of 3. Operating in a pulsed mode with electron beam pulse length 100 ms and duty cycle close to 0.1 allows us to overcome this limitation and operate with instantaneous powers in excess of 120 kW.

1.3. Vacuum system

Vacuum requirements in EBTS are justified by the need to have as low as possible an influx of background ions into the ion trap, because with the limited capacity of the ion trap these ions can replace the injected ions. Since background ions are typically lighter than injected ions, there can be some positive effect from these background ions: they can provide cooling of the injected ions. Ion cooling is desirable to keep ions within electron beam boundaries, thereby maintaining ionization efficiency and reducing the emittance of the extracted ion beam. It is advantageous to be able to inject cooling ions into the electron beam in a controlled way, so the intrinsic background pressure should be significantly lower than the pressure of the cooling species. An estimate of the time necessary to neutralize electron space charge ($\tau_{neut.}$) with nitrogen ions (residual gas component) made using the formula of E. Donets [6], gives $\tau_{neut.}$ = 4.5 s for pressure P=1x10^{-10} Torr and electron beam energy of E_{el}=10 keV. This is 45 times longer than the required confinement time for producing Au^{35+} ions, so the contribution of background ions to the total accumulated ion charge should not be higher than 2%. With residual gas pressure P=1x10^{-9} Torr the fraction of residual gas ions is expected to be less than 20%.

The required vacuum in EBTS is achieved with a "warm" vacuum system, using conventional vacuum technology. With a high power electron beam running, besides small current losses on electrodes, one of the major sources of residual gas is outgassing from the electron collector surface as a result of electron-stimulated desorption. The other source of outgassing in EBTS is from the electron gun. To reduce the flux of residual gas from the EC and gun into central chamber, both of these regions are connected to the central chamber with the smallest possible vacuum conductivity. Essentially, both the EC and electron gun chambers are connected to the central chamber through cross-sectional areas just slightly larger than that of electron beam. This concept of vacuum separation of the heavily outgassing end parts of EBTS from the central ion trap allows one to maintain a pressure in the central vacuum chamber 10 times lower than in the EC or gun chambers with the maximum running electron beam. Pressure in the central chamber improves with training of the EC by the electron beam. The EBTS vacuum system is presented in Fig. 9.

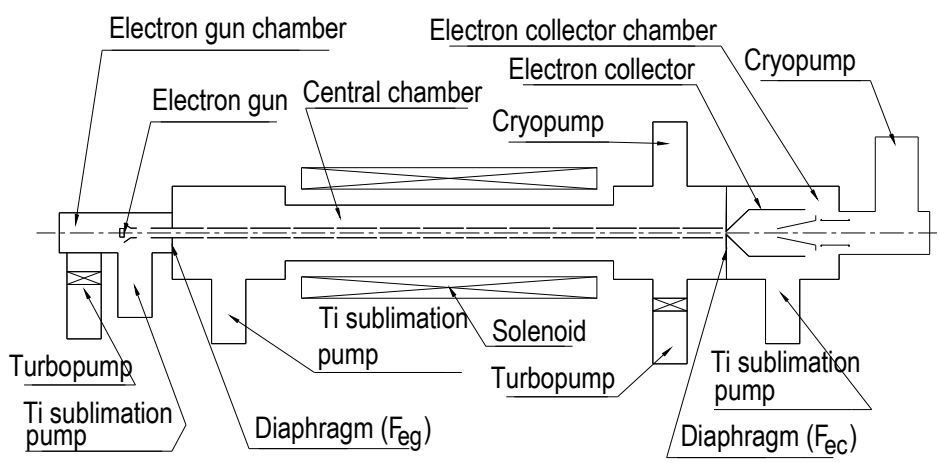

Fig. 9. Schematic diagram of the EBTS vacuum system

Total vacuum conductivity of both these chambers with the central chamber is $F_{eg}+F_{ec}\approx 100$ l/s.

As discussed in Section 1, one of the reasons for using an unshielded superconducting solenoid is to extend the electron beam path in order to connect standard vacuum pumps to the central vacuum chamber. While it may possible to use non-evaporating getters (NEG pumps) in the central region of EBTS, it was preferable in our present stage of R&D to have vacuum pumps with unlimited gas capacity. Typical pressure in the EBTS central chamber with a 7 A electron beam running at a duty cycle 0.1 is $1\text{-}2\times10^{-9}$ Torr. The local pressure in a region of the trap is probably somewhat higher than that measured with gauges on the sides of the central chamber. The pressure of residual gas decreased and $\tau_{neut.}$ increased several times after baking EBTS for 24÷48 hours with an average temperature of bakeout of 200^0C. The temperature limit for bakeout is caused by materials used to fix vacuum leaks.

2. EXPERIMENTAL RESULTS

First experiments with EBTS addressed transmission of multi-amp electron beams through the drift structure and dissipation of electron beam power on the electron collector. It was determined rather quickly, that one can transmit electron beam with very low losses with pulse duration of several milliseconds. Subsequent experiments focused on ion production and extraction, with operation with residual gas, with continuous gas injection and external ion injection.

2.1. Electron beam experiments

A multiampere electron beam was successfully transmitted through the drift structure of EBTS with low losses. Fig. 10 shows an electron beam with pulse length 5 ms and current 11 A, transmitted through the drift structure. Electron beam with current up to 8.6 A has been transmitted in 100 ms pulses. With proper adjustment of currents in the bucking and transverse magnet coils the electron beam loss is less than

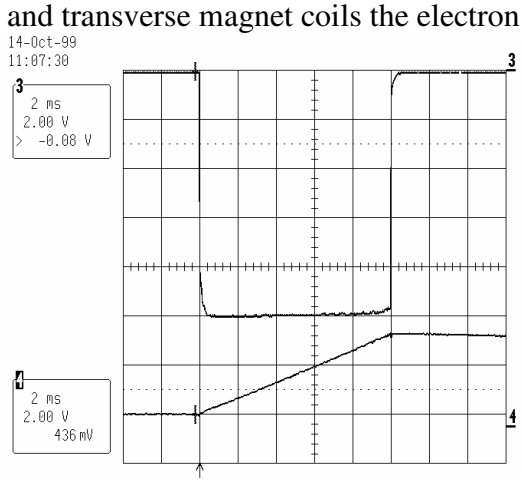

Fig. 10. Electron beam pulse of 11 A, 5 ms. Lower trace is a signal from infrared photo-diodes.

0.5 mA for a beam current up to 7 A, and is detected primarily on the 4 quadrants of the electron suppressor at the entrance of the EC. This level of losses did not have a

visible effect on $\tau_{neut.}$ so there was no need to apply negative voltage to the suppressor; instead, it was maintained at the same potential as the EC (ground). For 10 A electron current it was found that the minimum allowable potential difference of the electron collector with respect to the cathode is U_{EC-C}=10 kV, which corresponds to a maximum perveance $P_{EC}=10\cdot10^{-6}$. The minimum potential difference between the cathode and central drift tubes was found to be U_{DT-C}=28.2 kV. As the minimum potential U_{EC-C} is approached, but before a virtual cathode is evident, the electron beam develops oscillations with frequency 50 kHz and amplitude ~4%. The achieved minimum potentials on drift tubes and EC are somewhat higher than simulated and the difference can be explained by a higher temperature of the electron beam than assumed in simulations.

2.2. Continuous gas injection

2.2.1 Residual gas

Experiments on ionization of residual gas were made for electron beam currents up to 6 A. For I_{el}=6 A the potential difference between cathode and central drift tubes was 17.6 kV (that means the electron beam energy of was E_{el}=17.6 keV, assuming full compensation of the trap). The axial potential well applied to the drift tubes was ΔU_{trap}=4.6 kV. Neutralization time was $\tau_{neut.}$=10 ms. The high voltage pulse was applied to the central 4 drift tubes, that form the bottom of the ion trap through a resistor/capacitor network which induced a linear gradient of a few kV during ion extraction. Extracted ion current was measured on the first Faraday cup with 7 cm diameter, 70 cm from the EBTS exit. Secondary electrons were suppressed with voltage -200 V. An oscillogram of ion current on the first Faraday cup for τ_{conf}=10 ms is presented in Fig.11. As one can see, the maximum total ion current is I_{ion}=3.3 mA and FWHM of the ion pulse is τ_{ion_pulse}~10 μs. The total charge of extracted ions is Q_{ion}=30.5 nC (integral of ion current between two cursors in Fig. 11).

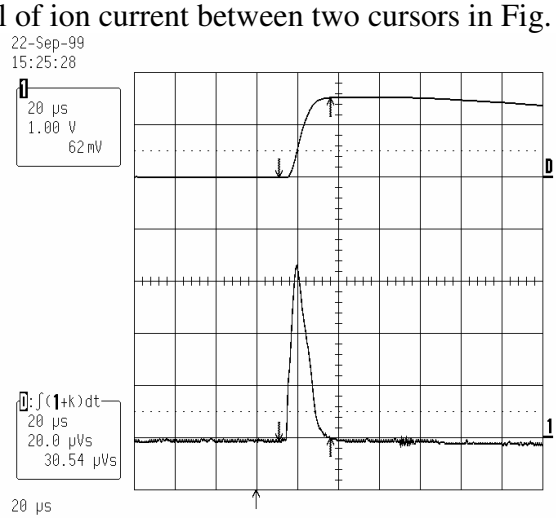

Fig. 11. Ion current signal (residual gas) from EBTS. I_{el}=6 A, E_e=17.6 keV, ΔU_{trap}=4.7 kV, τ_{conf}=10 ms. Lower trace – ion current (1 mA/div), upper trace – integral of ion current over time.

Since the capacity of ion trap (space charge of electrons in the volume of ion trap) is Q_{el}=53.6 nC, it means the neutralization of the ion trap (defined as $\eta=Q_{ion}/Q_{el}$), in this

experiment was η=57%. This result demonstrate the ability of an EBIS to compress its ion charge into an intense, short duration pulse.

2.2.2 Ionization of Ar and Xe

Even though the EBTS was not designed to operate with gas injection of the primary ion species, we found it instructive to experiment with gas injection. The EBTS does not have a convenient way to separate a gas injection region from the main ion trap region, such as is possible in cryogenic sources. Therefore, the injection becomes one of constant neutral density rather than fixed particle number, which would be preferable for obtaining intense beams with narrow spectra and high charge states. For continuous gas injection the equilibrium in the composition of the extracted ion beam is determined by the ratio of the partial pressure of the gas of interest (injected gas) to the residual gas pressure, and the ratio of their masses. The intensity of the extracted ion beam increases with increased gas pressure. On the other hand, the maximum ion charge state is determined by recombination effects and the time the ions spend in the beam, and this time becomes shorter with increased gas pressure. In our experiments, gas was injected continuously into the central chamber from a needle valve. A time of flight (TOF) spectrum of Ar ions with electron current I_{el}=1 A and confinement time τ_{conf}=40 ms is presented in Fig. 12. The maximum intensity line is Ar^{8+}. In this case the contribution of residual gas is relatively small. The efficiency of ionization, defined as the ratio of confinement time theoretically required to achieve this spectrum to the actual confinement time, is estimated to be ~25%. Total extracted ion charge measured on the first Faraday cup was Q_{ion}=8 nC and the capacity of ion trap was Q_{el}=10.35 nC. This ion yield corresponds to a

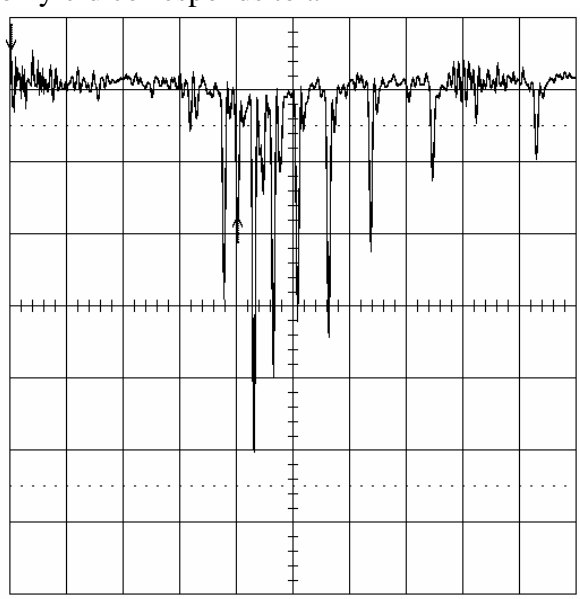

Fig. 12. TOF spectrum of Ar ions with I_{el}=1 A, τ_{conf}=40 ms, E_{el}=13.1 keV, ΔU_{trap}=1.1 kV. Cursor (arrow) is on Ar^{9+}.

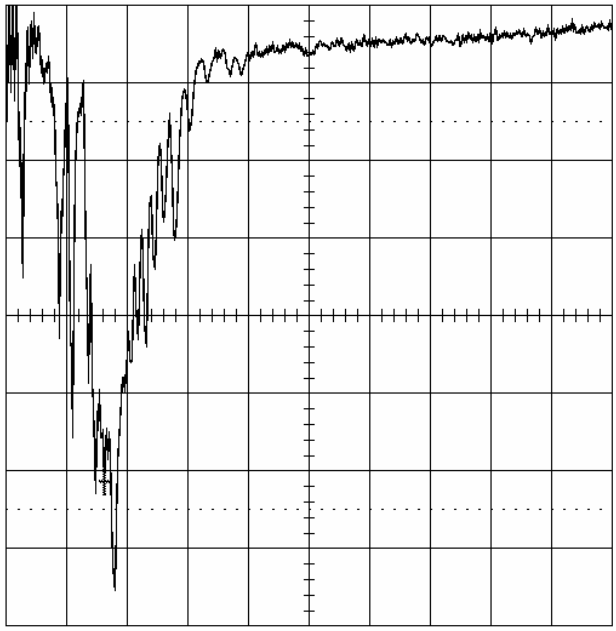

Fig. 13. TOF spectrum of Xe ions with I_{el}=4 A, τ_{conf}=20 ms, E_{el}=18.4 keV, ΔU_{trap}=4.0 kV. Cursor is on line Xe^{20+}.

neutralization of electron space charge with ions of η=77%. Similar experiments have been done with Xe, with an electron current up to 4.0 A. The charge state distribution of extracted ions with Xe injection is presented in Fig. 13. The contribution of residual gas in this spectrum is not dominating, but it is higher than in previous experiment with Ar, possibly because of a lower partial pressure of Xe. With a total ion yield Q_{ion}=13 nC, neutralization of the ion trap is η=37%, but the efficiency of ionization in this experiment is more than 50%.

As one can see, with continuous gas injection the efficiency of ionization depends on the pressure of gas, or more generally on the rate new ions are generated in the trap. With a higher rate of new ion generation the accumulated total ion charge is larger, but the average time spent in the electron beam by ions decreases, which means a lower efficiency of ionization. This behavior of EBTS corresponds to the basic phenomenological model of EBIS; for electron beam currents I_{el}>1 A on EBTS no significant difference have been observed compared to sources operating with I_{el}<1 A.

2.3 External ion injection

In experiments with external ion injection, singly charged Cs ions were injected into the trap from an auxiliary thermionic emission ion source. The Cs ion source was operated in a pulsed mode to have long emitter lifetime at high instantaneous current. Cs^{1+} beams with current up to 40 μA were extracted with pulse duration ranging from 200 μs to 2.5 ms. On the Faraday cup FC1, located close to the EBTS entrance, the current of Cs^{1+} ions was 15 μA. A schematic of EBTS external ion optics is presented in Fig. 14.

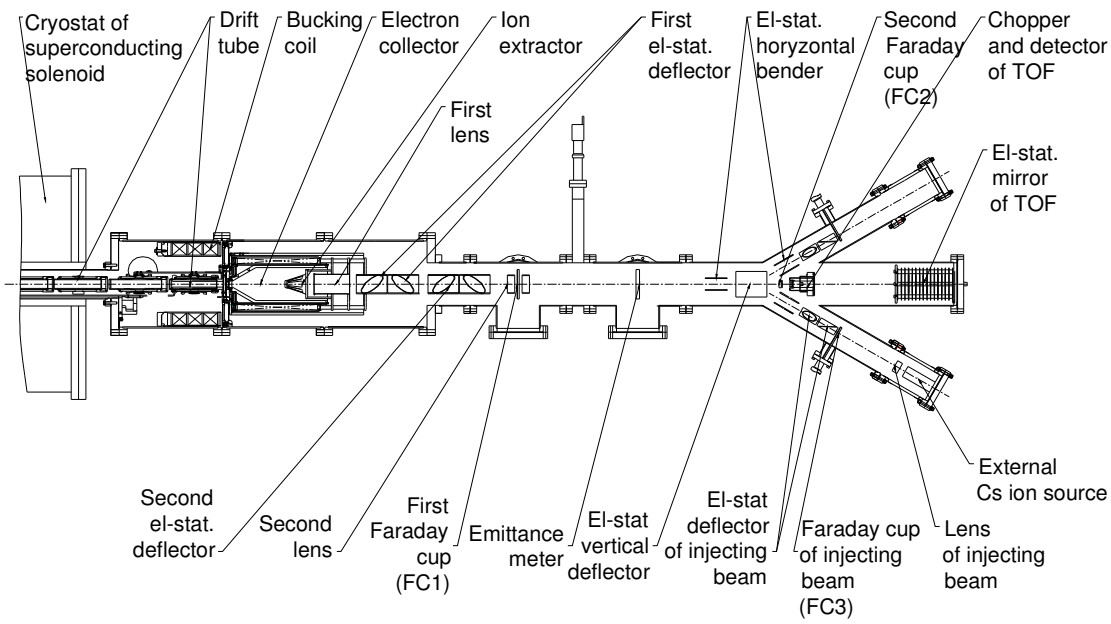

Fig. 14. EBTS external ion optics.

To inject efficiently, it is advantageous to retard the injected Cs^{1+} beam to <100 eV in the EBTS trap region, thereby increasing the linear Cs^{1+} charge density. Therefore, the Cs ion source was biased to +10 kV, approximately the potential of the EBTS trap region during injection, so the energy of Cs^{1+} ions in the transport beam line was E_{ion_inj}=10 keV.

The ion optical system, shown in Fig. 14, is used both for injection of ions from the auxiliary ion source and for diagnostics of the ion beam extracted from EBTS. The transport line includes 30° electrostatic deflectors, which allow use of multiple auxiliary sources and provide for time-of-flight (TOF) analysis of the extracted EBTS beam in the straight section. The injected ion beam was monitored with two removable Faraday cups: FC3 at the exit of Cs ion source in a side branch, and FC1 close to the exit from EBTS. The extracted ion beam from the EBTS was measured on FC2, located 160 cm from the exit of EBTS. The transport efficiency of extracted ion beams from FC1 to FC2 for these injection trials varied from 50÷90% depending on the magnitude of ion current extracted from EBTS.

Experiments on ion injection were performed in both slow and fast injection modes. In "slow" injection, Cs^{1+}ions were introduced into the trap over the extraction barrier, traversed the trap, were reflected from the barrier on the gun side of the trap, and returned back to the injection line, oscillating between reflecting potentials until hitting the wall. Only ions that increase their charge state through ionization by the electron beam between barriers get trapped. Since the probability of ionization is not very high, the process of filling the trap with injected ions in this way can take a long time. In this experiment, the maximum pulse length of ion current from the auxiliary ion source was 2.7 ms. After injection and confinement for 2 ms, ions where extracted from the trap and analyzed. With electron beam I_{el}= 1 A and E_{el}=16.5 keV, total ion charge measured on Faraday cup FC2 was Q_{ion}=0.6 nC, which corresponds to 6.5% neutralization of electron space charge in the trap. The fraction of Cs ions in the

spectrum of extracted ions was about 50% and the maximum intensity charge state was Cs^{8+}. The capture efficiency of Cs^{1+} ions, defined as a ratio of trapped ions measured after extraction on Faraday cup FC2 to number of incoming Cs ions, measured on Faraday cup FC1 was less than 1%.

In "fast" injection, with an initial flat potential distribution on trap drift tubes, ions of Cs^{1+} make a round trip traversal of the trap region, reflecting from the gun barrier. A flat potential distribution is imposed in the trap region and the potential can be adjusted to increase the linear charge density of the injected Cs^{1+} beam. With the Cs^{1+} ion beam present, the potential on the trap drift tubes is then lowered, resulting in axial trapping of traveling ions, which find themselves confined between two axial barriers. In this method of injection, ions do not have to be further ionized to be trapped; therefore the efficiency of trapping can be high and the injection times are rather short. For the present trial, the extracted ion intensity was maximized for τ_{inj}~200μs. This corresponds to a kinetic energy of Cs^{1+} ions in the trap region of ~35eV during injection. With electron beam parameters I_{el}=1.3 A, E_{el}=16 keV the total ion charge measured on Faraday cup FC2 after confinement time τ_{conf}=2 ms was Q_{ion}=2.45 nC and neutralization of the trap was η=20%. For residual gas pulses of comparable intensity, the transmission efficiency to FC2 from the EBTS exit is ~70%. If this transmission factor is taken into account, neutralization of the trap related to the exit of EBTS is η=29%. Efficiency of trapping ions, as defined above, in this case was 19% with respect to a 15 μA injected Cs^{1+} beam measured on FC1. An injection efficiency of >50% has been reported at the EBIS "DIONE" at Saclay for Nitrogen and Argon beams [7]. Since without ion injection very little charge of extracted ions was measured on Faraday cup FC2 after confinement time τ_{conf}=2 ms, one can say that the contribution of residual gas ions to the extracted ion beam is negligible. Oscillograms of extracted ion current on Faraday cup FC2 after confinement time τ_{conf}=2 ms with and without ion injection are presented in Fig. 15.

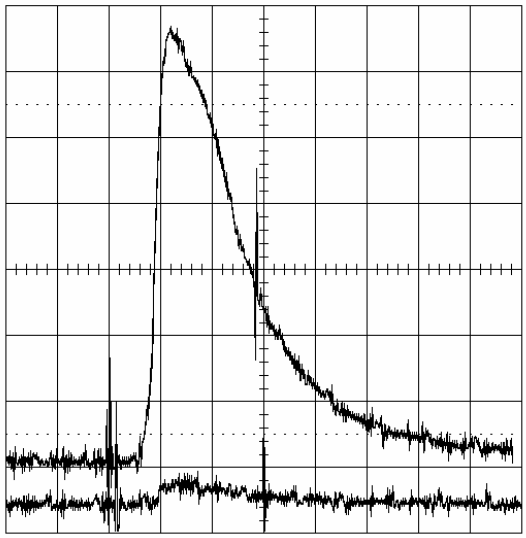

Fig. 15. Ion current pulses of on Faraday cup FC2 with (top trace) and without (bottom trace) Cs ion injection. I_{el}=1.3 keV, E_{el}=16 keV, τ_{conf}=2 ms. Scale: vertical – 10 μA/div., horizontal: 20 μs/div.

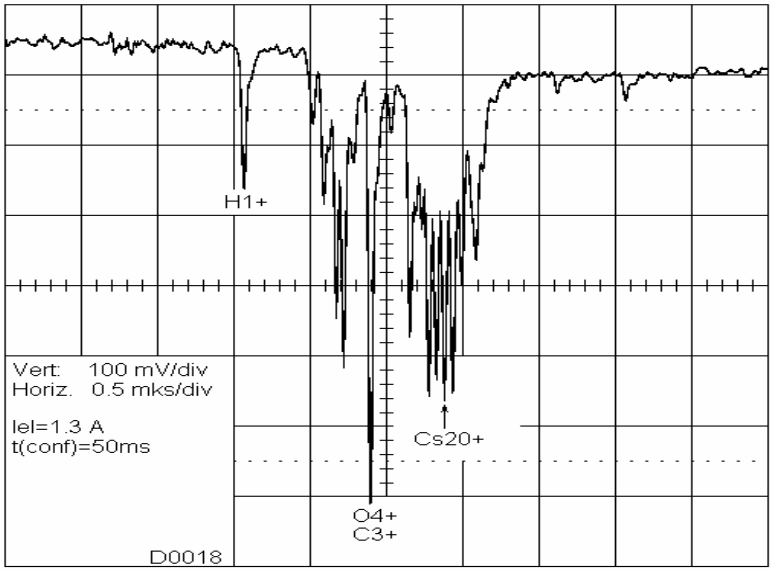

Fig. 16. TOF spectrum of extracted ion beam with Cs ion injection. I_{el}=1.3 A, E_{el}=16 keV, τ_{conf}=40 ms.

The charge state distribution of ions extracted from EBTS with electron beam I_{el}=1.3 A after confinement time τ_{conf}=40 ms is shown in Fig. 16.

With confinement time longer than 40 ms the fraction of residual gas ions (H, C and O) increases due to insufficient vacuum conditions existing because of a water leak and insufficient baking. The shape of the Cs ion charge state distribution is narrower than that of Xe ions with continuous gas injection: it contains less low charge state lines than with continuous injection; the Cs spectrum shows the advantage of the ideal pulsed ion injection.

The results of these experiments with external ion injection indicate that ions from the external ion source are injected into the EBTS ion trap with good efficiency. Fast ion injection is the preferable mode of injection at least for auxiliary ion sources with limited capacity. To increase EBTS intensity with external ion injection the intensity of auxiliary ion source should be increased and efficiency of ion transmission in the transport line should be improved. To reduce influx of residual gas ions into the trap, the vacuum in the trap region should be improved. This will be done by eliminating leaks and eliminating materials incompatible with proper baking. This will allow us to make better use of the pumps that have been installed, such as the titanium sublimators, and opens the possibility for pumping with NEG or additional cryopanels.

SUMMARY

Performance of the EBTS in experiments to date shows that the attained parameters (electron current, electron energy, vacuum and voltage range) are consistent with the project goals. The main result of these experiments is the demonstrated stability of the ion trap with multi-amp electron beams. Ions can be injected, confined and extracted just as in other EBISs or EBITs operating with currents below 1 A. Ion beams with total charge up to 30 nC and current more than 3 mA were extracted from EBTS,

indicating neutralization of the electron space charge by ions in the trap of more than 50%, and demonstrating fast ion extraction with pulse duration ~10 μs for residual gas. Experiments with EBTS indicate that its performance as a prototype for a future RHIC EBIS is on course to meet the design goals. It is left to show that we can produce the required number of ions in the charge state of interest for a heavy ion.

Further advances in EBTS performance will be associated with increased pulse duration of multi-ampere electron beams, improved vacuum conditions, and improved voltage holdoff in the drift tube region. Improvements to the control system, the ion injection system, experiments with solid injection, and improved ion transport of both injected and extracted beams are also expected to increase source performance.

ACKNOWLEDGEMENTS

*This work performed under the auspices of the US Department of Energy.
The authors would like to thank L. Liljeby, A. Hershcovitch, and R. Becker for fruitful discussions. We want to thank D. McCafferty, J. Ritter, O. Gould, and R. Schoepfer for their excellent technical support.

REFERENCES

1. K. Prelec, J. Alessi, and A. Hershcovitch, *Proceedings of Fourth European Particle Accelerator Conference*, London, (World Scientific, Singapore, 1994), p. 1435.
2. E. Beebe, J. Alessi, A. Hershcovitch, A. Kponou, A. Pikin, K. Prelec, and P. Stein *Review of Scientific Instruments*, V. 69, No. 2, Part II, 1998, p. 640.
3. A. Pikin, J. Alessi, E. Beebe, A. Kponou, K. Prelec,, and L. Snydstrup*, Review of Scientific Instruments*, V. 69, No. 2, Part II, 1998, p. 697.
4. A. Kponou, E. Beebe, A. Pikin, G. Kuznetsov, M. Batazova, and M. Tiunov, *Review of Scientific Instruments*, V. 69, No. 2, Part II, 1998, p. 1120.
5. B.M. Fomel, M.A. Tiunov, and V.P. Yakovlev, Report BINP No. 96-11, Novosibirsk, 1996.
6. E.Donets, in *The Physics and Technology of Ion Sources*, ed. Ian G.Brown (John Wiley & Sons, 1989), p. 249.
7. B. Visentine, P. Van Duppen, P.A. Leroy, R. Gobin, *Nuclear Instruments and Methods*, B101, 1995, p. 275.